RSC Advances

This article can be cited before page numbers have been issued, to do this please use: J. Shao, N. Fu, W. Yang, C. Zhang, Y. Zhong, Y. lin and J. Yao, *RSC Adv.*, 2015, DOI: 10.1039/C5RA20294A.

View Article Online
DOI: 10.1039/C5RA20294A

Journal Name

ARTICLE

Cyclometalated Ruthenium(II) Complexes with Bis(benzimidazolyl)benzene for Dye-Sensitized Solar Cells

Received 00th January 20xx,
Accepted 00th January 20xx

DOI: 10.1039/x0xx00000x

www.rsc.org/ra

Jiang-Yang Shao,[a] Nianqing Fu,[a] Wen-Wen Yang,[a] Chun-Yu Zhang,[a] Yu-Wu Zhong,*[a] Yuan Lin*[a] and Jiannian Yao[a]

A series of cyclometalated ruthenium complexes with the bis(benzimidazolyl)benzene ligand were prepared and their applications in dye-sensitized solar cells are presented. The Ru(III/II) redox process of these complexes occurs at +0.71 V vs Ag/AgCl. All complexes show broad absorptions extending into the near-infrared (NIR) region. The length of alkyl chains on the benzimidazole rings were found critical to the device performance. Sensitizer **4b** with octyl substituents exhibits the best cell performance under the standard air mass 1.5 sunlight (η = 3.7%, J_{sc} = 9.85 mA/cm^2, V_{oc} = 555 mV, FF = 0.67). The device exhibits appreciable action in the NIR region between 700 and 850 nm.

Introduction

Since the pioneering work by O'Regan and Grätzel in 1991,[1] dye-sensitized solar cells (DSSCs) have been extensively studied due to their low cost, easy fabrication, and high power conversion efficiency (η).[2] Recently, the record efficiency has been boosted to 13%.[3] Photosensitizers such as ruthenium complexes, zinc porphyrins, and metal-free organic dyes have been developed to serve as efficient light harvesters for DSSCs.[4] In spite of these efforts, new dyes have continued to be designed to broaden their light absorption wavelength range, increase molar absorptivity and improve the long-term stability of solar cells.[5]

Ruthenium(II) polypyridyl complexes are promising sensitizers for DSSCs. They display rich metal-to-ligand charge transfer (MLCT) absorptions in the visible region.[6] Many ruthenium sensitizers are known to achieve efficiencies higher than 10%, such as N3, N719, Z907, and black dyes.[7] However, the thiocyanate-containing ruthenium(II) complexes are questioned by the stability problems because the thiocyanate ligands are labile under thermal stress and long-term light soaking. This may hinder the commercialization prospect of DSSCs.[8] In this context, many attempts have been made to replace the thiocyanate ligands in ruthenium dyes.[9] For instance, Singh and co-workers reported a thiocyante-free ruthenium dye SPS-G3 containing the tridentate 2,6-bis(N-methylbenzimidazol-2-yl)pyridine ligand, with which an efficiency of 6.04% has been achieved.[10] It should be noted that most thiocyanate-free ruthenium complexes exhibit insufficient light harvesting in the near-infrared (NIR) region. Dyes that absorb in the NIR region are believed critical to further improve the cell efficiency, because NIR light accounts for a significant percentage of solar energy.[11]

Cyclometalated ruthenium complexes contain a Ru-C bond between the metal center and a supporting ligand.[12] Because of the presence of the carbon anionic ligand, the metal center of cyclometalated ruthenium complexes is much more electron-rich with respect to that of conventional trisbipyridine or bisterpyridine ruthenium complexes. The highest occupied molecular orbital (HOMO) and lowest unoccupied molecular orbital (LUMO) levels of cyclometalated ruthenium complexes can be largely modulated by changing the electronic nature of the cyclometalating ligand and noncyclometalating ligand, respectively. Recently, cyclometalated ruthenium(II) complexes have been shown to act as efficient sensitizers in DSSCs.[13] The elevated HOMO level of cyclometalated ruthenium complexes relative to trisbipyridine or bisterpyridine ruthenium complexes lead to a bathochromic shift of the absorption spectrum. On the other hand, the HOMO level of cyclometalated ruthenium complexes is still below the $I_2^{\bullet-}/I^-$ level, which ensures efficient dye regeneration. In addition, replacing the thiocyanate ligands of common ruthenium dyes with chelating cyclometalating ligands provides the opportunity to enhance the dye stability. The first example of a cyclometalated ruthenium sensitizer on TiO_2 was reported by van Koten and co-workers to produce a modest η of 2.1%.[14] In 2009, Grätzel and co-workers reported a η of 10.1% with a cyclometalated dye YE05.[15] Following these works, many new cyclometalated ruthenium dyes have been synthesized and studied.[16] However, cyclometalated ruthenium dyes that display efficient NIR absorptions are still limited.

[a] Beijing National Laboratory for Molecular Sciences, CAS Key Laboratory of Photochemistry, Institute of Chemistry, Chinese Academy of Sciences, Beijing 100190, China. *Email: zhongyuwu@iccas.ac.cn (Y.-W.Z.); linyuan@iccas.ac.cn (Y.L.).

Electronic Supplementary Information (ESI) available: CVs and DPVs of **1a**, **3a** – **5a**, photocurrent density-voltage characteristic of the device with N3, NMR and mass spectra of new compounds, and Cartesian coordinates for the DFT-optimized structure of **2a**$^+$. See DOI: 10.1039/x0xx00000x

View Article Online
DOI: 10.1039/C5RA20294A

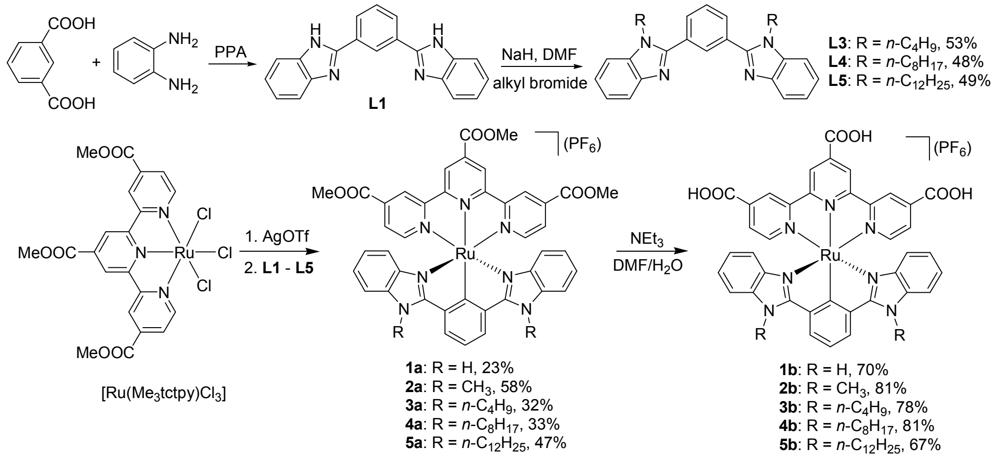

Scheme 1 Synthesis of Compounds **1b** – **5b**

We report herein the synthesis and characterization of five cyclometalated ruthenium(II) dyes (**1b** - **5b**) with the bis(benzimidazolyl)benzene ligand (Scheme 1). Proton or alkyl chains of various lengths are placed on the benzimidazole rings. All complexes show broad absorptions extending into the NIR region. The DSSC performances of these complexes on TiO_2 and the effect of the length of alkyl chains on the device performance are presented. It should be noted that although the effect alkyl chains on DSSC performance has been reported,[7i,7j] this effect has not been examined on cyclometalated ruthenium dyes.

Results and discussion

Synthesis

Ruthenium dyes **1b** – **5b** were synthesized as outlined in Scheme 1. Ligands 1,3-bis(2-benzimidazolyl)benzene (**L1**), 1,3-bis(N-methylbenzimidazolyl)benzene (**L2**) and 1,3-bis(N-butylbenzimidazolyl)benzene (**L3**) were synthesized according to literature procedures.[17] The reaction of isophthalic acid with 1,2-diaminobenzene or N-methyl-1,2-benzenediamine dihydrochloride in polyphosphoric acid (PPA) afforded **L1** and **L2**, respectively. The N-alkylated derivatives of **L1**, namely **L3**, 1,3-bis(N-octylbenzimidazolyl)benzene (**L4**), and 1,3-bis(N-dodecylbenzimidazolyl)benzene (**L5**), were prepared by deprotonation of **L1** with NaH, followed by subsequent alkylation with 1-bromobutane, 1-bromooctane and 1-bromododecane, respectively. Cyclometalated ruthenium complexes **1a** – **5a** were prepared by the reaction of [Ru(Me_3tctpy)Cl_3] (Me_3tctpy = trimethyl-4,4',4''-tricarboxylate-2,2':6',2''-terpyridine) with ligands **L1** – **L5** respectively, in the presence of AgOTf, followed by anion exchange using KPF_6. These complexes were purified through flash column chromatography on silica gel and obtained as bench-stable compounds. The reaction of **1a** – **5a** with triethylamine in a mixed solvent of DMF and H_2O gave the ruthenium complexes **1b** – **5b**. These products were purified by column chromatography on silica gel with 5 mM tetrabutylammonium hydroxide (TBAOH) in methanol/water (1:1, v/v) as the eluent. The isolated solid was obtained as the TBA salt at this stage. This salt was then dissolved in water, followed the addition of 1 M aqueous HCl. The resulting precipitate was isolated to afford complexes **1b** – **5b** in acceptable yield. The identity of cyclometalated ruthenium complexes with one PF_6^- counteranion is supported by microanalysis data. This differs from [RuN_6]-type noncyclometalated ruthenium complexes which needs the presence of two counteranions.

Single crystal of **2a** suitable for X-ray analysis was obtained by diffusion of petroleum ether into the solution of the complex in CH_2Cl_2. The thermal ellipsoid plot of the X-ray structure is shown in Fig. 1. The ruthenium ion has an expected octahedral configuration with one NNN- and one NCN-type tridentate ligand. The Ru-C bond has a distance of 2.009(6) Å.

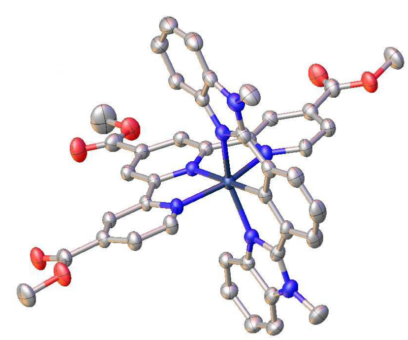

Fig. 1 Thermal ellipsoid plot of the single-crystal X-ray structure of **2a** at 30% probability. Solvents and anion (PF_6^-) are omitted for clarity.

Electrochemical Studies and Density Functional Theory (DFT) Calculation

The electronic properties of **1a** – **5a** were examined by cyclic voltammetric (CV) studies. The anodic CV of **1a** – **5a** in CH_3CN are shown in Fig. 2a. All complexes exhibit a

View Article Online
DOI: 10.1039/C5RA20294A

chemically reversible redox couple at +0.71 V vs Ag/AgCl (+0.26 V vs the ferrocene/ferrocenium redox couple). These waves are ascribed to the $Ru^{III/II}$ process with some possible involvement of the oxidation of the cyclometalating ring. Note that the $Ru^{III/II}$ potential of $[RuN_6]$-type noncyclometalated ruthenium complexes generally occurs around +1.3 V vs Ag/AgCl.[12d] The HOMO energy level of **1a** – **5a** is estimated to be +0.91 V with respect to a normal hydrogen electrode (NHE) and the dyes **1b** – **5b** on TiO_2 are believed to have similar HOMO energy levels. This suggests that the dye can be efficiently regenerated by I^- ($E(I_2^{\bullet-}/I^-)$ = +0.79 V vs NHE in CH_3CN).[18] The second oxidation waves of complexes **1a** – **5a** around +1.60 V vs Ag/AgCl are ascribed to the $Ru^{IV/III}$ process (Fig. 2b and S1 – S4 in the Supporting Information, SI). Taking complex **2a** as an example (Fig. 2b), two chemically reversible cathodic waves are observed at −1.10 and −1.45 V vs Ag/AgCl (−1.55 and −1.90 V vs ferrocene/ferrocenium). These waves are assigned to the reductions of the noncyclometalating ligand (Me_3tctpy). A previously reported cyclometalated ruthenium complex [Ru(Me_3tctpy)(dpb)](PF_6) (dpb = 1,3-di(pyrid-2-yl)benzene) also shows two cathodic waves at −1.10 and −1.45 V vs Ag/AgCl.[19,20]

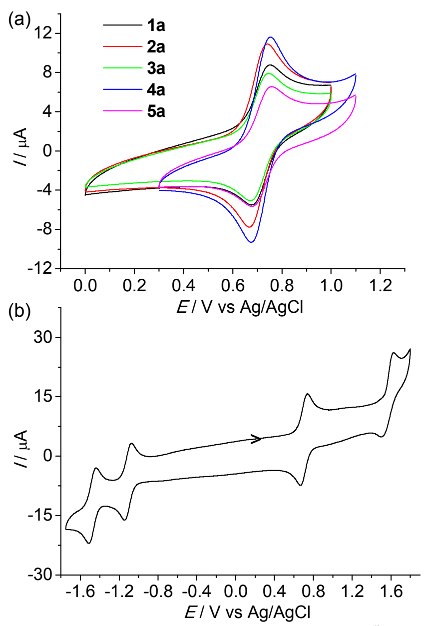

Fig. 2 (a) CVs of **1a** – **5a** in CH_3CN containing 0.1 M ^{n}Bu$_4$NClO$_4$ as the supporting electrolyte at a scan rate of 100 mV/s. The working electrode is a glassy carbon and the counter electrode is a platinum wire. The reference electrode is Ag/AgCl in saturated aqueous NaCl solution. (b) CV of **2a** in CH_3CN in a wide potential window.

DFT calculations were performed on **2a** on the level of theory of B3LYP/6-31G*/LANL2DZ. Fig. 3 shows the isodensity plots of selected frontier orbitals of **2a** along with the energy level label. The HOMO of **2a** exhibits a high electron delocalization between ruthenium and the cyclometalating ligand. This phenomenon is commonly observed in the DFT results of cyclometalated ruthenium complexes.[20] This suggests that the first oxidation event of **2a** is mostly associated with the ruthenium ion and the metalating phenyl ring as has been mentioned above. The HOMO-1 and HOMO-2 of **2a** are dominated by the ruthenium ion. The LUMO, LUMO+1 and LUMO+2 are associated with the noncyclometalating ligand, which suggests that the terpyridine ligand is mostly involved in the first reduction event of **2a**.

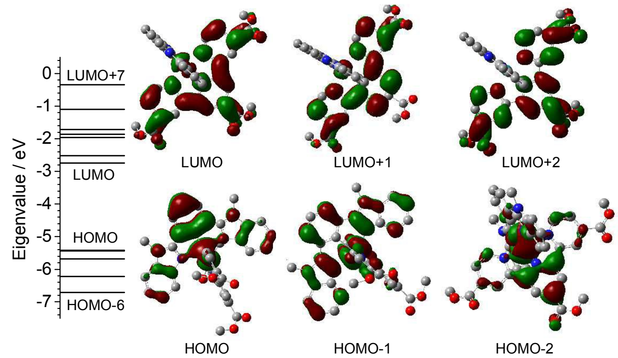

Fig. 3 Isodensity plots of selected frontier orbitals of **2a** along with the energy level label.

Electronic Absorption Spectra and Time-Dependent DFT (TDDFT) Calculations

The electronic absorption spectra of complexes **1a** – **5a** are shown in Fig. 4, together with that of N3 for comparison. Complexes **1a** – **5a** exhibit very similar absorption patterns and molar absorptivity. The absorptions in the ultraviolet (UV) region are due to intraligand transitions from both cyclometalating and auxiliary ligands. In the visible (vis) to NIR region, three main absorption bands are distinguished (350 ~ 500 nm; 500 ~ 650 nm; 650 ~ 900 nm), which are largely ascribed to the MLCT transitions. In addition, these complexes display distinct absorptions in the wavelength range of 700 ~ 900 nm. This feature is not observed for N3 and the previously reported ruthenium dye with the noncyclometalating 2,6-bis(*N*-methylbenzimidazol-2-yl)pyridine ligand SPS-G3.[10] No distinct emission was recorded for these complexes at room temperature. Cyclometalated ruthenium complexes are known to be non- or very weakly emissive.[16k]

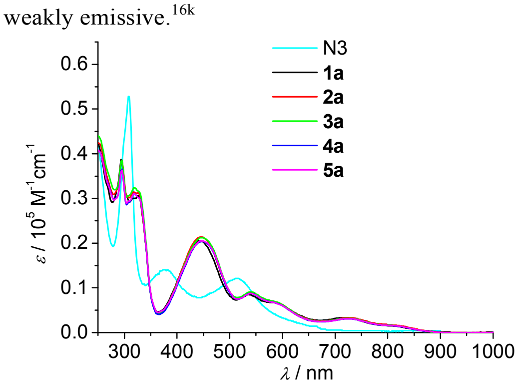

Fig. 4 UV/vis absorption spectra of **1a** – **5a** and N3.

View Article Online
DOI: 10.1039/C5RA20294A

In order to assist the detailed interpretations of the absorption bands of these complexes, TDDFT calculations were performed on complex **2a** on the basis of the above DFT-optimized structure. The predicted main low-energy excitations are shown in Fig. 5**,** and related results are summarized in Table 1. TDDFT results suggest that the absorption bands between 650 and 900 nm are mainly associated with the HOMO-1 → LUMO transition (S_2 excitation). The predicted S_5 and S_6 excitations of complex **2a** at 519 and 493 nm are responsible for the experimentally observed absorptions between 500 and 650 nm. These two excitations are associated with the excitation of HOMO-2 → LUMO+1 and HOMO-2 → LUMO, respectively. A series of excitations in 350 ~ 500 nm region with appreciable oscillator strengths are predicted (from S_9 to S_{20} excitations). These excitations are associated with the charge transfer from the HOMO, HOMO-1, HOMO-2, and HOMO-3 orbitals of complex **2a**.

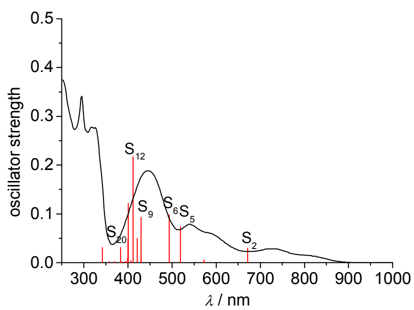

Fig. 5 UV/vis absorption spectrum (black curve) and TDDFT-predicted excitations (vertical red lines) of **2a**.

Table 1 Calculated Excitation Energy (*E*), Oscillator Strength (*f*), Dominant Contributing Transitions and Associated Percent Contribution of **2a**

S_n	*E* / eV	*λ* / nm	*f*	dominant transitions
2	1.85	671	0.0297	HOMO-1 → LUMO (95%)
5	2.39	519	0.0736	HOMO-2 → LUMO+1 (97%)
6	2.51	493	0.0978	HOMO-2 → LUMO (50%)
9	2.89	430	0.0929	HOMO-1 → LUMO+2 (69%)
10	2.89	429	0.0129	HOMO → LUMO+3 (83%)
11	2.94	421	0.0495	HOMO-3 → LUMO (78%)
12	3.01	411	0.2166	HOMO → LUMO+4 (94%)
14	3.09	401	0.1215	HOMO-2 → LUMO+2 (42%)
15	3.10	400	0.0495	HOMO-2 → LUMO+3 (75%)
20	3.23	383	0.0306	HOMO-3 → LUMO+1 (78%)

Photovoltaic Performance

In order to evaluate the performance of ruthenium(II) complexes in the DSSCs, commercially available test cells with transparent TiO_2 anodes stained with the standard N3 dye or the cyclometalated ruthenium dyes **1b** – **5b** were assembled according to standard literature procedures.[21] The photovoltaic properties were measured using the liquid electrolyte containing 0.5 M LiI, 0.05 M I_2, 0.6 M 4-*tert*-butylpyridine (TBP), and 0.6 M 1-methyl-3-hexylimidazolium iodide (HMII) in 3-methoxypropionitrile (MPN) under AM 1.5 full sunlight (100 mW/cm^2) illumination. Their typical photocurrent density–voltage (*J*-V) characteristics are shown in Fig. 6 and Table 2.

Among the five cyclometalated ruthenium dyes studied, **4b** shows the best photovoltaic performance, which exhibits an open-circuit photovoltage (V_{oc}) of 555 mV, a short-circuit photocurrent density (J_{sc}) of 9.85 mA/cm^2, a fill-factor (*FF*) of 0.67, and η of 3.7%, respectively. Under similar conditions, the N3-sensitized device gave a V_{oc} of 625 mV, J_{sc} of 12.56 mA/cm^2, *FF* of 0.69, and η of 5.4% (Fig. S5). The length of alkyl chains is critical for the performance of the cells using **1b** – **5b**. The short circuit current density increases with increasing length of alkyl chains from **1b** through **4b**. These alkyl chains form a molecular layer with high hydrophobicity between the mesoporous TiO_2 surface and the electrolyte, which is beneficial for reducing the electron-hole recombination.[22] However, the cell with the dodecyl-substituted dye **5b** shows a reduced J_{sc} of 8.56 mA/cm^2 with respect to the octyl-substituted dye **4b**. In this case, the dye regeneration may be retarded due to the thick alkyl layer, leading to the reduced device performance. The open-circuit photovoltage consistently increases with increasing length of alkyl chains from **1b** through **5b**. The power conversion efficiency of **1b**, **2b**, **3b**, and **5b** is 0.8%, 1.5%, 2.3%, and 3.3%, respectively.

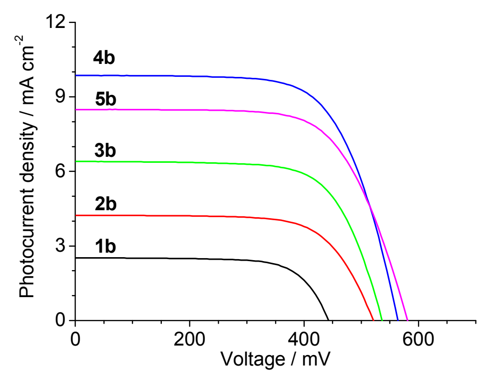

Fig. 6 Photocurrent density-voltage characteristic of devices using cyclometalated ruthenium sensitizers.

Table 2 Photovoltaic properties of DSSCs.

Dye	J_{sc} (mA/cm^2)	V_{oc} (mV)	η (%)	*FF*
N3	12.56	625	5.4	0.69
1b	2.47	435	0.8	0.70
2b	4.19	510	1.5	0.69
3b	6.39	530	2.3	0.68
4b	9.85	555	3.7	0.67
5b	8.56	575	3.3	0.66

View Article Online
DOI: 10.1039/C5RA20294A

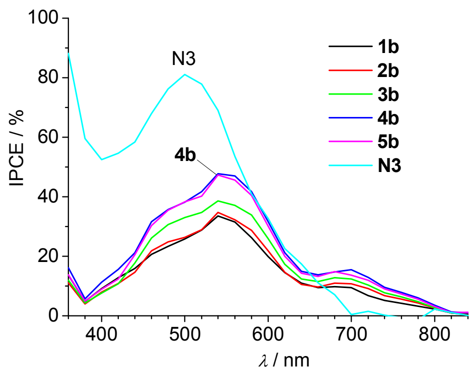

Fig. 7 The IPCE characteristics of DSSCs with **1b** – **5b** and N3.

The incident photon-to-current conversion efficiency (IPCE) characteristics of the devices using the above ruthenium dyes and N3 are shown in Fig. 7. The maximum IPCE of **4**b occur around 530 nm (48.0%). All devices exhibit appreciable actions in the region between 700 and 850 nm. The device with **4**b shows an IPCE of 15.5% at 700 nm. In contrast, the device with N3 shows no photo action in this region. We believe that the absorption of these cyclometalated ruthenium dyes can be further extended into longer-wavelength region by structural modifications.

Conclusions

To summarize, five cyclometalated ruthenium(II) complexes based on the bis(benzimidazolyl)benzene ligand with varying alkyl chains were prepared. These complexes show absorptions in a wide range of wavelength extending into the NIR region. The dye-sensitized solar cells with these complexes on TiO_2 were investigated. The best power conversion efficiencies of 3.7% was achieved with the dye with octyl substituents. This result indicates that dyes with appropriate length of alkyl chains are critical for the optimization of device performance. Cyclometalated ruthenium complexes are potential dyes for harvesting the NIR light, which is important for further improvement of the power conversion efficiency of DSSC.

Experimental

Spectroscopic and Electrochemical Measurements. All optical ultraviolet/visible (UV/vis) absorption spectra were obtained using a TU-1810DSPC spectrometer of Beijing Purkinje General Instrument Co. Ltd. at room temperature in denoted solvents, with a conventional 1.0 cm quartz cell. All cyclic voltammograms were taken using a CHI 620D or 660D potentiostat. All measurements were carried out in 0.1 M of Bu_4NClO_4/CH_3CN at a scan rate of 100 mV/s with a Ag/AgCl reference electrode. The working electrode was glassy carbon, and a platinum coil was used as the counter electrode.

Computational Methods. DFT calculations were carried out using the B3LYP exchange correlation functional[23] and implemented in the Gaussian 09 package. The electronic structures of complexes were determined using a general basis set with the Los Alamos effective core potential LANL2DZ basis set for ruthenium and 6-31G* for other atoms.[24] In all calculations, solvation effects in CH_3CN are included, and the conductor-like polarizable continuum model (CPCM) was employed.[25] All orbitals have been computed at an isovalue of 0.02 e/bohr^3.

Fabrication of DSSCs. The solar cells were fabricated and measured according to known procedures.[26] TiO_2 was fabricated on the FTO substrates (fluorine-doped SnO_2, 15 Ω/sq) using a doctor-blade method and the electrodes were heated at 450 °C for 30 min. After this sintering, the temperature was cooled to 90 °C. The electrodes were then immersed in a dye bath (3×10^{-4} M) in ethanol for 24 h. The redox electrolyte is a mixture of 0.5 M LiI, 0.05 M I_2, 0.6 M TBP, and 0.6 M HMII in MPN. The counter electrode is Pt-coated FTO. The sandwiched solar cells were assembled using the dye-sensitized TiO_2 photoelectrode and the Pt counter electrode with the liquid electrolyte between them.

Photovoltaic Measurements. The photocurrent density-voltage (*J*-V) measurements were tested using a Keithley 2611 Source Meter. The light source is an AM 1.5 solar simulator (91160A, Newport Co.). The incident light intensity is 100 mW/cm^2 calibrated with a standard Si solar cell. The tested solar cells have a working area of 0.2 cm^2.

X-ray Crystallography. The X-ray diffraction data were collected using a Rigaku Saturn 724 diffractometer on a rotating anode (Mo-K radiation, 0.71073 Å) at 173 K. The structure was solved by the direct method using SHELXS-97[27] and refined with SHELXT-2014[28] in conjugation with Olex2.[29] Crystallographic data for **2a** (CCDC 1428503): $C_{43}H_{34}F_6N_7O_6PRu{\cdot}3.5(CH_2Cl_2)$, M = 1288.05, triclinic, space group P-1, a = 12.163(3), b = 13.716(3), c = 18.215(4) Å, α = 105.644(2)º, β = 94.048(2)º, γ = 115.759(2)º, U = 2572.8(9) Å^3, T = 173 K, Z = 2, 31799 reflections measured, radiation type MoK\a, radiation wavelength 0.71073 Å, final R indices R1 = 0.0688, wR2 = 0.1717, R indices (all data) R1 = 0.0736, wR2 = 0.1754.

Synthesis. NMR spectra were recorded in the designated solvent on Bruker Avance 300 or 400 MHz spectrometer. Spectra are reported in ppm values from residual protons of deuterated solvent. Mass data were obtained with a Bruker Daltonics Inc. Apex II FT-ICR or Autoflex III MALDI-TOF mass spectrometer. The matrix for MALDI-TOF measurement is α-cyano-4-hydroxycinnamic acid. Microanalysis was carried out using Flash EA 1112 or Carlo Erba 1106 analyzer at the Institute of Chemistry, Chinese Academy of Sciences. Ligands **L1**, **L2** and **L3** were prepared according to the previously reported procedure.[17]

Synthesis of L4. To a solution of 1,3-bis(benzimidazolyl)benzene (100 mg, 0.32 mmol) and NaH (17 mg, 0.7 mmol) in 10 mL DMF was added 1-bromooctane (0.15 mL, 0.7 mmol). The resulting mixture was stirred at 100 °C for overnight under a nitrogen atmosphere. The solvent was removed in vacuum. The residue was dissolved in 10 mL CH_2Cl_2, followed by washing with water (3 × 30 mL) and drying over anhydrous $MgSO_4$. After filtration and removal of the solvent, the residue was purified by column chromatography on silica gel using petroleum ether/ethyl acetate (4/1, v/v) as the eluent to give 82 mg of L4 as a yellow oil in 48% yield. ^{1}H NMR (400 MHz, $CDCl_3$): δ 0.82 (t, J = 7.0 Hz, 6H), 1.17-

View Article Online
DOI: 10.1039/C5RA20294A

1.22 (m, 20H), 1.81 (t, J = 6.6 Hz, 4H), 4.26 (t, J = 7.6 Hz, 4H), 7.26-7.31 (m, 4H), 7.40-7.43 (m, 2H), 7.69 (t, J = 7.6 Hz, 1H), 7.81-7.84 (m, 2H), 7.88 (d, J = 7.6 Hz, 2H), 8.05 (s, 1H). ^{13}C NMR (100 MHz, $CDCl_3$): δ 8.17, 16.68, 20.83, 23.17, 23.97, 25.77, 39.04, 70.90, 71.21, 71.53, 104.4, 114.2, 116.6, 117.0, 123.4, 124.2, 124.7, 125.5, 129.7, 137.3, 146.9. HRMS (EI) calcd for $C_{36}H_{46}N_4$: 534.3722. Found: 534.3716.

Synthesis of L5. According to the synthetic procedure for L4, compound L5 was prepared from 1,3-bis(benzimidazolyl)benzene (103 mg, 0.32 mmol) and 1-bromododecane (0.16 mL, 0.7 mmol) in 49% yield. ^{1}H NMR (400 MHz, $CDCl_3$): δ 0.86 (t, J = 6.8 Hz, 6H), 1.17-1.22 (m, 36H), 1.81 (t, J = 6.4 Hz, 4H), 4.26 (t, J = 7.6 Hz, 4H), 7.29-7.33 (m, 4H), 7.43-7.44 (m, 2H), 7.69 (t, J = 7.6 Hz, 1H), 7.82-7.84 (m, 2H), 7.88 (d, J = 7.6 Hz, 2H), 8.05 (s, 1H). ^{13}C NMR (100 MHz, $CDCl_3$): δ 8.26, 16.81, 20.84, 23.19, 23.45, 23.54, 23.58, 23.70, 23.97, 26.02, 39.03, 70.91, 71.23, 71.55, 104.4, 114.2, 116.6, 117.0, 123.4, 124.2, 124.7, 125.5, 129.7 137.3, 146.9. HRMS (EI) calcd for $C_{44}H_{62}N_4$: 646.4974. Found: 646.4982.

Synthesis of Complex 1a. To 10 mL dry acetone were added [Ru(Me_3tctpy)Cl_3] (34 mg, 0.055 mmol) and AgOTf (58 mg, 0.23 mmol). The mixture was refluxed for 2 h before cooling to room temperature. The precipitate was removed by filtration, and the filtrate was concentrated to dryness. To the residue were added L1 (17 mg, 0.055 mmol), DMF (10 mL), and *t*-BuOH (10 mL). The mixture was then refluxed for 24 h. After cooling to room temperature, the solvent was removed under reduced pressure, and the residue was dissolved in proper amount of methanol. After addition of an excess of KPF_6, the resulting precipitate was collected by filtration and washing with water and Et_2O. The obtained solid was subjected to flash column chromatography on silica gel (eluent: CH_2Cl_2/ethyl acetate, 10/1) to give 11.3 mg complex 1a as a black solid in 23% yield. ^{1}H NMR (400 MHz, CD_3CN): δ 3.83 (s, 6H), 4.24 (s, 3H), 5.64 (d, J = 8.0 Hz, 2H), 6.72 (t, J = 7.6 Hz, 2H), 7.01 (t, J = 7.8 Hz, 2H), 7.36 (d, J = 8.4 Hz, 2H), 7.43 (s, 4H), 7.64 (t, J = 7.8 Hz, 1H), 8.24 (d, J = 7.6 Hz, 2H), 8.92 (s, 2H), 9.45 (s, 2H). ^{13}C NMR (100 MHz, CD_3CN): δ 52.73, 53.06, 112.5, 113.8, 122.1, 122.4, 123.1, 123.5, 123.6, 125.9, 132.2, 132.9, 133.2, 135.5, 142.1, 154.9, 155.7, 160.1, 161.5, 164.2, 165.6, 216.4. MALDI-TOF: 818.0 for $[M – PF_6]^+$. Anal. Calcd for $C_{41}H_{30}F_6N_7O_6PRu$: C, 51.15; H, 3.14; N, 10.18. Found: C, 50.95; H, 3.60; N, 9.79.

Synthesis of Complex 2a. According to the synthetic procedure for 1a, complex 2a was prepared from [Ru(Me_3tctpy)Cl_3] (37.4 mg, 0.06 mmol) and L2 (24.6 mg, 0.07 mmol) in 58% yield. ^{1}H NMR (400 MHz, CD_3CN): δ 3.83 (s, 6H), 4.24 (s, 3H), 4.30 (s, 6H), 5.60 (d, J = 8.0 Hz, 2H), 6.73 (t, J = 8.0 Hz, 2H), 7.06 (t, J = 8.0 Hz, 2H), 7.37 (d, J = 8.4 Hz, 2H), 7.44 (s, 4H), 7.64 (t, J = 8.0 Hz, 1H), 8.45 (d, J = 8.0 Hz, 2H), 8.91 (s, 2H), 9.46 (s, 2H). ^{13}C NMR (100 MHz, CD_3CN): δ 32.02, 52.73, 53.06, 54.51, 110.9, 113.7, 122.1, 122.4, 123.1, 123.2, 125.0, 125.8, 132.1, 134.1, 135.2, 135.4, 141.4, 154.7, 155.8, 160.0, 161.1, 164.2, 165.6, 218.9. MALDI-TOF: 846.6 for $[M – PF_6]^+$. Anal. Calcd for $C_{43}H_{34}F_6N_7O_6PRu$: C, 52.13; H, 3.46; N, 9.90. Found: C, 51.64; H, 3.44; N, 9.51.

Synthesis of Complex 3a. According to the synthetic procedure for 1a, complex 3a was prepared from [Ru(Me_3tctpy)Cl_3] (34 mg, 0.055 mmol) and L3 (30 mg, 0.07 mmol) in 32% yield. ^{1}H NMR (400 MHz, CD_3CN): δ 0.96 (t, J = 7.4 Hz, 6H), 1.41-1.48 (m, 4H), 1.96-2.04 (m, 4H), 3.83 (s, 6H), 4.23 (s, 3H), 4.73 (t, J = 7.6 Hz, 4H), 5.60 (d, J = 8.0 Hz, 2H), 6.74 (t, J = 7.8 Hz, 2H), 7.05 (t, J = 7.6 Hz, 2H), 7.39-7.44 (m, 6H), 7.67 (t, J = 7.6 Hz, 1H), 8.35 (d, J = 7.6 Hz, 2H), 8.92 (s, 2H), 9.46 (s, 2H). MALDI-TOF: 930.2 for $[M – PF_6]^+$. Anal. Calcd for $C_{49}H_{46}F_6N_7O_6PRu·H_2O$: C, 53.85; H, 4.43; N, 8.97. Found: C, 53.44; H, 4.27; N, 9.15.

Synthesis of Complex 4a. According to the synthetic procedure for 1a, complex 4a was prepared from [Ru(Me_3tctpy)Cl_3] (57 mg, 0.092 mmol) and L4 (54 mg, 0.1 mmol) in 33% yield. ^{1}H NMR (400 MHz, CD_3CN): δ 0.80 (t, J = 6.8 Hz, 6H), 1.16-1.27 (m, 20H), 1.35-1.41 (m, 4H), 3.83 (s, 6H), 4.24 (s, 3H), 4.73 (t, J = 7.0 Hz, 4H), 5.59 (d, J = 8.0 Hz, 2H), 6.73 (t, J = 7.6 Hz, 2H), 7.05 (t, J = 7.4 Hz, 2H), 7.38-7.42 (m, 6H), 7.65 (t, J = 7.2 Hz, 1H), 8.35 (d, J = 7.6 Hz, 2H), 8.92 (s, 2H), 9.46 (s, 2H). ^{13}C NMR (100 MHz, CD_3CN): δ 13.91, 22.84, 26.92, 29.40, 29.45, 30.03, 31.94, 45.48, 53.13, 53.46, 111.5, 114.2, 122.5, 122.9, 123.6, 123.7, 125.2, 126.3, 132.6, 134.1, 135.2, 135.8, 141.8, 155.0, 155.9, 160.3, 160.7, 164.5, 165.9, 219.6. MALDI-TOF: 1042.3 for $[M – PF_6]^+$. Anal. Calcd for $C_{57}H_{62}F_6N_7O_6PRu·H_2O$: C, 56.80; H, 5.35; N, 8.14. Found: C, 56.99; H, 5.26; N, 8.21.

Synthesis of Complex 5a. According to the synthetic procedure for 1a, complex 5a was prepared from [Ru(Me_3tctpy)Cl_3] (32 mg, 0.052 mmol) and L5 (35 mg, 0.054 mmol) in 47% yield. ^{1}H NMR (400 MHz, CD_3CN): δ 0.86 (t, J = 7.2 Hz, 6H), 1.10-1.28 (m, 36H), 1.33-1.41 (m, 4H), 3.83 (s, 6H), 4.24 (s, 3H), 4.73 (t, J = 7.2 Hz, 4H), 5.59 (d, J = 8.4 Hz, 2H), 6.73 (t, J = 7.6 Hz, 2H), 7.05 (t, J = 7.6 Hz, 2H), 7.38-7.42 (m, 6H), 7.65 (t, J = 8.0 Hz, 1H), 8.34 (d, J = 8.0 Hz, 2H), 8.92 (s, 2H), 9.46 (s, 2H). ^{13}C NMR (100 MHz, CD_3CN): δ 13.61, 22.60, 26.44, 29.00, 29.22, 29.42, 29.48, 29.54, 31.83, 45.10, 52.75, 53.07, 54.52, 111.2, 113.8, 122.2, 122.5, 123.3, 124.9, 125.9, 132.2, 133.7, 134.9, 135.4, 141.4, 154.7, 155.6, 159.9, 160.3, 164.1, 165.5, 219.2. MALDI-TOF: 1154.4 for $[M – PF_6]^+$. Anal. Calcd for $C_{65}H_{78}F_6N_7O_6PRu·H_2O$: C, 59.26; H, 6.12; N, 7.44. Found: C, 59.13; H, 6.12; N, 7.43.

Synthesis of Complex 1b. A solution of 1a (15 mg, 0.016 mmol), H_2O (5 mL), and NEt_3 (5 mL) in 20 mL DMF was refluxed for 24 h. After cooling to room temperature, the solvent was removed under reduced pressure. The residue was dissolved in a minimal amount of 0.1 M tetrabutylammonium hydroxide (TBAOH) in methanol/H_2O (1:1, v/v). The product was purified by column chromatography on silica gel with 5 mM TBAOH in methanol/water (1:1, v/v) as the eluent. The isolated solid was dissolved in proper amount water followed by the addition of 0.1 M aqueous HCl. The resulting precipitate was filtrated, and washed with water to give 10 mg complex 1b in 70% yield. ^{1}H NMR (400 MHz, CD_3OD): δ 5.73 (d, J = 8.4 Hz, 2H), 6.69 (t, J = 7.8 Hz, 2H), 6.97 (t, J = 7.6 Hz, 2H), 7.23 (d, J = 6.0 Hz, 2H), 7.31 (t, J = 7.2 Hz, 4H), 7.54 (t, J = 7.6 Hz, 1H), 8.20 (d, J = 7.6 Hz, 2H), 8.86 (s, 2H), 9.40 (s, 2H). MALDI-TOF: 775.9 for $[M – PF_6]^+$. Anal. Calcd for $C_{38}H_{24}F_6N_7O_6PRu$: C, 49.57; H, 2.63; N, 10.65. Found: C, 50.01; H, 3.20; N, 10.95.

Synthesis of Complex 2b. According to the synthetic procedure for 1b, complex 2b was prepared from 2a (13.3 mg, 0.013 mmol) in

View Article Online
DOI: 10.1039/C5RA20294A

81% yield. ^{1}H NMR (400 MHz, CD_3OD): δ 4.38 (s, 6H), 5.73 (d, J = 8.0 Hz, 2H), 6.73 (t, J = 7.6 Hz, 2H), 7.04 (t, J = 7.4 Hz, 2H), 7.21 (d, J = 6.0 Hz, 2H), 7.28 (d, J = 6.4 Hz, 2H), 7.39 (d, J = 8.4 Hz, 2H), 7.61 (t, J = 7.8 Hz, 1H), 8.48 (d, J = 8.0 Hz, 2H), 8.84 (s, 2H), 9.39 (s, 2H). MALDI-TOF: 804.2 for $[M - PF_6]^+$. Anal. Calcd for $C_{40}H_{28}F_6N_7O_6PRu{\cdot}H_2O$: C, 49.70; H, 3.13; N, 10.14. Found: C, 49.13; H, 3.66; N, 10.51.

Synthesis of Complex 3b. According to the synthetic procedure for 1b, complex 3b was prepared from 3a (15 mg, 0.014 mmol) in 78% yield. ^{1}H NMR (400 MHz, d_6-DMSO): δ 0.88 (t, J = 7.2 Hz, 6H), 1.34-1.40 (m, 4H), 1.90-1.93 (m, 4H), 4.84 (s, 4H), 5.53 (d, J = 8.4 Hz, 2H), 6.80 (t, J = 7.8 Hz, 2H), 7.07 (t, J = 7.4 Hz, 2H), 7.31 (d, J = 5.6 Hz, 2H), 7.53 (d, J = 5.6 Hz, 2H), 7.61 (d, J = 8.0 Hz, 2H), 7.68 (t, J = 7.8 Hz, 1H), 8.42 (d, J = 7.6 Hz, 2H), 9.14 (s, 2H), 9.69 (s, 2H). MALDI-TOF: 887.8 for $[M - PF_6]^+$. Anal. Calcd for $C_{46}H_{40}F_6N_7O_6PRu{\cdot}H_2O$: C, 52.57; H, 4.03; N, 9.33. Found: C, 52.63; H, 4.52; N, 9.13.

Synthesis of Complex 4b. According to the synthetic procedure for 1b, complex 4b was prepared from 4a (15 mg, 0.013 mmol) in 81% yield. ^{1}H NMR (400 MHz, d_6-DMSO): δ 0.73 (t, J = 8.8 Hz, 6H), 1.05-1.23 (m, 20H), 1.93-1.96 (m, 4H), 4.85 (s, 4H), 5.52 (d, J = 10.4 Hz, 2H), 6.79 (t, J = 10.2 Hz, 2H), 7.06 (t, J = 9.6 Hz, 2H), 7.31 (d, J = 7.6 Hz, 2H), 7.50 (d, J = 7.6 Hz, 2H), 7.63 (m, 3H), 8.42 (d, J = 7.6 Hz, 2H), 9.14 (s, 2H), 9.69 (s, 2H). MALDI-TOF: 999.9 for $[M - PF_6]^+$. Anal. Calcd for $C_{54}H_{56}F_6N_7O_6PRu$: C, 56.64; H, 4.93; N, 8.56. Found: C, 56.80; H, 5.26; N, 8.21.

Synthesis of Complex 5b. According to the synthetic procedure for 1b, complex 5b was prepared from 5a (15 mg, 0.012 mmol) in 67% yield. ^{1}H NMR (400 MHz, d_6-DMSO): δ 0.95 (t, J = 8.6 Hz, 6H), 1.04-1.28 (m, 36H), 1.92-19.5 (m, 4H), 4.85 (s, 4H), 5.52 (d, J = 8.0 Hz, 2H), 6.78 (t, J = 7.6 Hz, 2H), 7.06 (t, J = 7.6 Hz, 2H), 7.31 (d, J = 5.6 Hz, 2H), 7.50 (d, J = 7.6 Hz, 2H), 7.64 (m, 3H), 8.42 (d, J = 8.0 Hz, 2H), 9.14 (s, 2H), 9.69 (s, 2H). MALDI-TOF: 1112.3 for $[M - PF_6]^+$. Anal. Calcd for $C_{62}H_{72}F_6N_7O_6PRu{\cdot}H_2O$: C, 58.39; H, 5.85; N, 7.69. Found: C, 58.08; H, 5.66; N, 7.17.

Acknowledgements.

We thank the National Natural Science Foundation of China (grants 21501183, 91227104, 21271176, 21472196, and 21221002), the Ministry of Science and Technology of China (grant 2012YQ120060), the Strategic Priority Research Program of the Chinese Academy of Sciences (grant XDB 12010400), and Institute of Chemistry, Chinese Academy of Sciences (grant PY-201524) for funding support.

Notes and references

1 B. O'Regan and M. Grätzel, *Nature,* 1991, **353**, 737.
2 L. El Chaar and N. El Zein, *Renew. Sustain. Energy Rev.,* 2011, **15**, 2165.
3 S. Mathew, A. Yella, P. Gao, R. Humphry-Baker, B. F. E. Curchod, N. Ashari-Astani, I. Tavernelli, U. Rothlisberger, M. K. Nazeeruddin and M. Grätzel, *Nat. Chem.,* 2014, **6**, 242.
4 (a) Q. Yu, Y. Wang, Z. Yi, N. Zu, J. Zhang, M. Zhang and P. Wang, *ACS Nano,* 2010, **4**, 6032; (b) A. Yella, H. W. Lee, H. N. Tsao, C. Yi, A. K. Chandiran, M. K. Nazeeruddin, E. W. G. Diau, C. Y. Yeh, S. M. Zakeeruddin and M. Grätzel, *Science,* 2011, **334**, 629; (c) A. Yella, R. Humphry-Baker, B. F. E. Curchod, N. Ashari-Astani, J. Teuscher, L. E. Polander, S. Mathew, J.-E. Moser, I. Tavernelli, U. Rothlisberger, M. Grätzel, Md. K. Nazeeruddin and J. Frey, *Chem. Mater.,* 2013, **25**, 2733; (d) P. G. Bomben, B. D. Koivisto and C. P. Berlinguette, *Inorg. Chem.,* 2010, **49**, 4960.
5 (a) S.-W. Wang, K.-L. Wu, E. Ghadiri, M. G. Lobello, S.-T. Ho, Y. Chi, J.-E. Moser, F. De Angelis, M. Grätzel and M. K. Nazeeruddin, *Chem. Sci.,* 2013, **4**, 2423; (b) T. Moehl, H. N. Tsao, K.-L. Wu, H.-C. Hsu, Y. Chi, E. Ronca, F. De Angelis, M. K. Nazeeruddin and M. Grätzel, *Chem. Mater.,* 2013, **25**, 4497; (c) J. Zheng, T.-L. Zhang, X.-F. Zang, D.-B. Kuang, H. Meier and D.-R. Cao, *Sci. China Chem.,* 2013, **56**, 505; (d) C.-C. Chou, F.-C. Hu, H.-H. Yeh, H.-P. Wu, Y. Chi, J. N. Clifford, E. Palomares, S.-H. Liu, P.-T. Chou and G.-H. Lee, *Angew. Chem. Int. Ed.,* 2014, **53**, 178; (e) K. Kanaizuka, S. Yagyu, A. Kajikawa, T. Kakuta, H. Kon, T. Togashi, K. Uruma, M. Ishizaki, M. Sakamoto and M. Kurihara, *Chem. Lett.,* 2013, **42**, 669. (f) L.-J. Wang, K. Zhang, F.-Y. Cheng and J. Chen, *Sci. China Chem.,* 2014, **57**, 1559.
6 (a) J.-F. Yin, M. Velayudham, D. Bhattacharya, H.-C. Lin and K.-L. Lu, *Coord. Chem. Rev.,* 2012, **256**, 3008; (b) A. Juris, V. Balzani, F. Barigelletti, S. Campagna, P. Belser and A. von Zelewsky, *Coord. Chem. Rev.,* 1988, **84**, 85; (c) G. C. Vougioukalakis, A. I. Philippopoulous, T. Stergiopoulos and P. Falaras, *Coord. Chem. Rev.,* 2011, **255**, 2602; (d) H. Ozawa, K. Fukushima, T. Sugiura, A. Urayama and H. Arakawa, *Dalton. Trans.,* 2014, **43**, 13208; (e) B.-B. Ma, Y.-X. Peng, T. Tao and W. Huang, *Dalton. Trans.,* 2014, **43**, 16601; (f) H. Ozawa, T. Kuroda, S. Harada and H. Arakawa, *Eur. J. Inorg. Chem.,* 2014, 4734; (g) C.-C. Chou, F.-C. Hu, K.-L. Wu, T. Duan, Y. Chi, S.-H. Liu, G.-H. Lee and P.-T. Chou, *Inorg. Chem.,* 2014, **53**, 8593; (h) C. Dragonetti, A. Colombo, M. Magni, P. Mussini, F. Nisic, D. Roberto, R. Ugo, A. Valore, A. Valsecchi, P. Salvatori, M. G. Lobello and F. D. Angelis, *Inorg. Chem.,* 2013, **52**, 10723.
7 (a) M. K. Nazeeruddin, F. De Angelis, S. Fantacci, A. Selloni, G. Viscardi, P. Liska, S. Ito, B. Takeru and M. Grätzel, *J. Am. Chem. Soc.,* 2005, **127**, 16835; (b) A. Islam, T. Swetha, M. R. Karim, Md. Akhtaruzzaman, L. Han and S. P. Singh, *Phys. Status Solidi A,* 2015, **3**, 651; (c) K. C. D. Robson, P. G. Bomben and C. P. Berlinguette, *Dalton Trans.,* 2012, **41**, 7814; (d) M. K. Nazeeruddin, A. Kay, I. Rodicio, R. Humpbry-Baker, E. Muller, P. Liska, N. Vlachopoulos and M. Grätzel, *J. Am. Chem. Soc.,* 1993, **115**, 6382; (e) M. Y. A. Rahman, A. A. Umar, R. Taslim and M. M. Salleh, *Electrochim. Acta,* 2013, **88**, 639. (f) Q. Yu, S. Liu, M. Zhang, N. Cai, Y. Wang and P. Wang, *J. Phys. Chem. C,* 2009, **113**, 14559; (g) M. Wang, S.-J. Moon, D. Zhou, F. Le Formal, N.-L. Cevey-Ha, R. Humphry-Baker, C. Grätzel, P. Wang, S. M. Zakeeruddin and M. Grätzel, *Adv. Funct. Mater.,* 2010, **20**, 1821; (h) S.-H. Yang, K.-L. Wu, Y. Chi, Y.-M. Cheng and P.-T. Chou, *Angew. Chem. Int. Ed.,* 2011, **50**, 8270; (i) S. N. Mori, W. Kubo, T. Kanzaki, N. Masaki, Y. Wada and S. Yanagida, *J. Phys. Chem. C,* 2007, **111**, 3522; (j) Y.-S. Yen, Y.-

View Article Online
DOI: 10.1039/C5RA20294A

C. Chen, Y.-C. Hsu, H.-H. Chou, J. T. Lin and D.-J. Yin, *Chem. Eur. J.,* 2011, **17**, 6781.

8 (a) O. Kohle, M. Grätzel, A. F. Meyer and T. B. Meyer, *Adv. Mater.,* 1997, **9**, 904; (b) P. T. Nguyen, A. R. Andersen, E. M. Skou and T. Lund, *Sol. Energy Mater. Sol. Cells,* 2010, **94**, 1582; (c) Y. Numata, S. P. Singh, A. Islam, M. Iwamura, A. Imai, K. Nozaki and L. Han, *Adv. Funct. Mater.,* 2013, **23**, 1817; (d) D. G. Brown, P. A. Schauer, J. Borau-Garcia, B. R. Fancy and C. P. Berlinguette, *J. Am. Chem. Soc.,* 2013, **135**, 1692.

9 (a) P. T. Nguyen, B. X. T. Lam, A. R. Andersen, P. E. Hansen and T. Lund, *Eur. J. Inorg. Chem.,* 2011, 2533; (b) C. Dragonetti, A. Colombo, M. Magni, P. Mussini, F. Nisic, D. Roberto, R. Ugo, A. Valore, A. Valsecchi, P. Salvatori, M. G. Lobello and F. D. Angelis, *Inorg. Chem.,* 2013, **52**, 10723; (c) S. Sinn, B. Schulze, C. Friebe, D. G. Brown, M. Jäger, J. Kübel, B. Dietzek, C. P. Berlinguette and U. S. Schubert, *Inorg. Chem.,* 2014, **53**, 1637. (d) H. C. Zhao, J. P. Harney, Y.-T. Huang, J.-H. Yum, M. K. Nazeeruddin, M. Grätzel, M.-K. Tsai and J. Rochford, *Inorg. Chem.*, 2012, **51**, 1; (e) K.-L. Wu, Y. Hu, C.-T. Chao, Y.-W. Yang, T.-Y. Hsiao, N. Robertson and Y. Chi, *J. Mater. Chem. A*, 2014, **2**, 19556.

10 S. P. Singh, K. S. V. Gupta, M. Chandrasekharam, A. Islam, L. Han, S. Yoshikawa, M. Haga, M. S. Roy and G. D. Sharma, *ACS Appl. Mater. Interfaces,* 2013, **5**, 11623.

11 (a) A. Hagfeldt, G. Boschloo, L. Sun, L. Kloo and H. Petterson, *Chem. Rev.,* 2010, 6595; (b) G. Li, A. Yella, D. G. Brown, S. I. Gorelsky, M. K. Nazeeruddin, M. Grätzel, C. P. Berlinguette and M. Shatruk, *Inorg. Chem.,* 2014, **53**, 5417; (c) C.-P. Lee, R. Y.-Y. Lin, L.-Y. Lin, C.-T. Li, T.-C. Chu, S.-S. Sun, J. T. Lin and K.-C. Ho, *RSC Adv.,* 2015, **5**, 23810.

12 (a) J.-Y. Shao, J. Yao, Y.-W. Zhong, *Organometallics,* 2012, **31**, 4302; (b) W.-W. Yang, Y.-W. Zhong, S. Yoshikawa, J.-Y. Shao, S. Masaoka, K. Sakai, J. Yao and M. Haga, *Inorg. Chem.,* 2012, **51**, 890; (c) J.-P. Djukic, J.-B. Sortais, L. Barloy and M. Pfeffer, *Eur. J. Inorg. Chem.,* 2009, 817; (d) W.-W. Yang, L. Wang, Y.-W. Zhong and J. Yao, *Organometallics,* 2011, **30**, 2236.

13 S. Soman, Y. Xie and T. W. Hamann, *Polyhedron,* 2014, **82**, 139.

14 S. H. Wadman, J. M. Kroon, K. Bakker, M. Lutz, A. L. Spek, G. P. M. van Klink and G. van Koten, *Chem. Commun.,* 2007, **4**, 1907.

15 (a) T. Bessho, E. Yoneda, J.-H. Yum, M. Guglielmi, I. Tavernelli, H. Imai, U. Rothlisberger, M. Nazeeruddin and M. Grätzel, *J. Am. Chem. Soc.,* 2009, **131**, 5930. (b) F. De Angelis, S. Fantacci, A. Selloni, M. K. Nazeeruddin and M. Gratzel, *J. Phys. Chem. C,* 2010, **114**, 6054.

16 (a) P. G. Bomben, K. C. D. Robson, B. D. Koivisto and C. P. Berlinguette, *Coord. Chem. Rev.,* 2012, **256**, 1438; (b) G. Li, P. G. Bomben, K. C. D. Robson, S. I. Gorelsky, C. P. Berlinguette and M. Shatruk, *Chem. Commun.,* 2012, **48**, 8790; (c) T. Swetha, S. Niveditha, K. Bhanuprakash and S. P. Singh, *Electrochim. Acta,* 2015, **153**, 343; (d) T. Funaki, H. Kusama, N. Onozawa-Komatsuzaki, K. Kasuga, K. Sayama and H. Sugihara, *Eur. J. Inorg. Chem.,* 2014, 1303; (e) Z. Huang, M. He, M. Yu, K. Click, D. Beauchamp and Y. Wu, *Angew. Chem. Int. Ed.,* 2015, **54**, 6857; (f) L. E. Polander, A. Yella, B. F. E. Curchod, N. A. Astani, J. Teuscher, R. Scopelliti, P. Gao, S. Mathew, J.-E. Moser, I. Tavernelli, U. Rothlisberger, M. Grätzel, Md. K. Nazeeruddin and J. Frey, *Angew. Chem. Int. Ed.,* 2013, **52**, 8731; (g) J.-J. Kim, H. Choi, S. Paek, C. Kim, K. Lim, M.-J. Ju, H. S. Kang, M.-S. Kang and J. Ko, *Inorg. Chem.,* 2011, **50**, 11340; (h) Y. Chi, K.-L. Wu and T.-C. Wei, *Chem. Asian J.,* 2015, **10**, 1098; (i) A. Abbotto, C. Coluccini, E. Dell'Orto, N. Manfredi, V. Trifiletti, M. M. Salamone, R. Ruffo, M. Acciarri, A. Colombo, C. Dragonetti, S. Ordanini, D. Roberto and A. Valore, *Dalton Trans.,* 2012, **41**, 11731; (j) H. Kisserwan, A. Kamar, T. Shoker and T. H. Ghaddar, *Dalton Trans.,* 2012, **41**, 10643. (k) K. C. D. Robson, B. Sporinova, B. D. Koivisto, E. Schott, D. G. Brown and C. P. Berlinguette, *Inorg. Chem.,* 2011, **50**, 6019.

17 (a) Y. Xu, J. Tang, G. Chang, X. Luo, F. Zhu and L. Zhang, *Chem. Asian J.,* 2013, **25**, 4013; (b) T. Yutaka, S. Obara, S. Ogawa, K. Nozaki, N. Ikeda, T. Ohno, Y. Ishii, K. Sakai and M. Haga, *Inorg. Chem.,* 2005, **44**, 4737; (c) W. Wu, J. Zhao, H. Guo, J. Sun, S. Ji and Z. Wang, *Chem. Eur. J.,* 2012, **18**, 1961.

18 G. Boschloo, E. A. Gibson and A. Hagfeldt, *J. Phys. Chem. Lett.,* 2011, **2**, 3016.

19 W.-W. Yang, J.-Y. Shao and Y.-W. Zhong, *Eur. J. Inorg. Chem.,* 2015, 3195.

20 (a) C.-J. Yao, H.-J. Nie, W.-W. Yang, J. Yao and Y.-W. Zhong, *Inorg. Chem.,* 2015, **54**, 4688; (b) C.-J. Yao, H.-J. Nie, W.-W. Yang, J.-Y. Shao, J. Yao and Y.-W. Zhong, *Chem. Eur. J.,* 2014, **20**, 17466.

21 (a) N. Q. Fu, X. R. Xiao, X. W. Zhou, J. B. Zhang and Y. Lin, *J. Phys. Chem. C,* 2012, **116**, 2850; (b) H.-J. Park, K. H. Kim, S. Y. Choi, H.-M. Kim, W. I. Lee, Y. K. Kang and Y. K. Chung, *Inorg. Chem.,* 2010, **49**, 7340; (c) S. Sinn, B. Schulze, C. Friebe, D. G. Brown, M. Jager, E. Altuntas, J. Kubel, O. Guntner, C. P. Berlinguette, B. Dietzek and U. S. Schubert, *Inorg. Chem.,* 2014, **53**, 2083.

22 (a) J. E. Kroeze, N. Hirata, S. Koops, M. K. Nazeeruddin, L. Schmidt-Mende, M. Grätzel and J. R. Durrant, *J. Am. Chem. Soc.,* 2006, **128**, 16376; (b) J.-S. Ni, C.-Y. Hung, K.-Y. Liu, Y.-H. Chang, K.-C. Ho and K.-F. Lin, *J. Colloid Interface Sci.,* 2012, **386**, 359; (c) W. H. Nguyen, C. D. Bailie, J. Burschka, T. Moehl, M. Grätzel, M. D. McGehee and A. Sellinger, *Chem. Mater.,* 2013, **25**, 1519; (d) W.-K. Huang, H.-P. Wu, P.-L. Lin and E. W.-G. Diau, *J. Phys. Chem. C,* 2013, **117**, 2059; (e) X. Xue, W. Zhang, N. Zhang, C. Ju, X. Peng, Y. Yang, Y. Liang, Y. Feng and B. Zhang, *RSC Adv.,* 2014, **4**, 8894.

23 C. Lee, W. Yang and R. G. Parr, *Phys. Rev. B,* 1988, **37**, 785.

24 P. J. Hay and W. R. Wadt, *J. Chem. Phys.,* 1985, **82**, 299.

25 V. Barone and M. Cossi, *J. Phys. Chem. A,* 1998, **102**, 1995.

26 (a) Z. Wan, C. Jia, Y. Duan, L. Zhou, Y. Lin and Y. Shi, *J. Mater. Chem.,* 2012, **22**, 25140; (b) Z. Wan, C. Jia, Y. Duan, X. Chen, Z. Li and Y. Liu, *RSC Adv.,* 2014, **4**, 34896.

27 G. M. Sheldrick, *Acta Cryst.*, 2008, **A64**, 112.

28 G. M. Sheldrick, *Acta Cryst.*, 2015, **A71**, 3.

29 O. V. Dolomanov, L. J. Bourhis, R. J. Gildea, J. A. K. Howard and H. Puschmann, *J. Appl. Cryst.*, 2009, **42**, 339.

View Article Online
DOI: 10.1039/C5RA20294A

Title/Authours/Abstract/Figure for Table of contents

Cyclometalated Ruthenium(II) Complexes with Bis(benzimidazolyl)benzene for Dye-Sensitized Solar Cells

Jiang-Yang Shao, Nianqing Fu, Wen-Wen Yang, Chun-Yu Zhang, Yu-Wu Zhong,* Yuan Lin* and Jiannian Yao

The length of alkyl chains on the benzimidazole rings of cyclometalated ruthenium dyes is critical to the DSSC performance.